

THE APPLICATION OF PULSED THERMOGRAPHY IMAGE PROCESSING METHOD TO LONGWAVE BOLOMETRIC INFRARED CAMERAS

Lovre, **Krstulović-Opara**, University of Split, Faculty of Electrical Engineering, Mechanical Engineering and Naval Architecture, Split, CROATIA, Lovre.Krstulovic-Opara@fesb.hr

Mislav, **Ljubenković**, University of Split, Faculty of Electrical Engineering, Mechanical Engineering and Naval Architecture, Split, CROATIA, mljubenk@fesb.hr

Željko, **Domazet**, University of Split, Faculty of Electrical Engineering, Mechanical Engineering and Naval Architecture, Split, CROATIA, Zeljko.Domazet@fesb.hr

ABSTRACT - Pulsed infrared thermography is a NDT method for evaluating polymer reinforced structures. As our former research was performed on advantageous cooled middle-wave camera, in this contribution gradient based image processing method has been applied on long-wave bolometric cameras. Different wavelengths and camera sensitivities have been compared on prefabricated specimen. To demonstrate the capability of approach, examples from floating vehicles industry have been presented.

Keywords: non-destructive testing, infrared thermography, bolometric cameras

1. INTRODUCTION

Thermography, as a non-destructive testing (NDT) method, is used mostly as passive observing method for evaluating structures and materials such as reinforced polymers. It is already a standard procedure performing passive thermographic inspection on aircrafts after landing, where search for ice inclusions due to the interlaminar humidity penetration is performed [1]. For such applications mostly bolometric long-wave (LW) infrared (IR) thermal cameras are used. Active thermography is mostly used in research [2 to 10] and in some advanced industries as a quality control system, e.g. wind turbine [11] and aircraft [12] industry. For such applications mostly cooled middle-wave (MW) cameras and halogen or Xenon lamps, as heat source, are used. Reason for using more expensive MW thermal imaging cameras is sensitivity (mostly 0.02°C) and high frame rates capable of capturing dynamic changes in heat flow. We have performed extensive research based on cooled MW IR camera with InSb detector and active pulsed thermography (PT), as well as pulsed phase thermograph (PPT) approach [13 to 17]. When comparing two basic groups of IR cameras; MW have

high frame rate (up to 700 Hz), high sensitivity ($0.02\pm 0.015^{\circ}\text{C}$) and high price, making them laboratory stationary equipment. LW IR cameras are characterized by lower frame rates (around 60 Hz) and lower sensitivity ($0.1\pm 0.05^{\circ}\text{C}$). LW cameras, due to lower price and ease to handle, are more often used in praxis and research. To promote active IR thermographic NDT for LW camera users, presented research is an application of knowledge obtained in the field of MW IR thermography to the field LW IR cameras. The idea is without having expensive MW IR cameras and IR research software, it should be possible to use same PT or PPT approaches with cheaper LW cameras, avoiding need for research software that provides IR image in a raw data format. Raw data field of temperatures is exported in matrix form, which can be mathematically modified afterwards. We have used standard Matlab routines to extract matrix of temperatures from JPEG image, which is a common output format of IR cameras. Temperatures, represented as a grayscale image level in matrix format, can be mathematically processed by known PT image processing methods used in NDT evaluation.

2. IMAGE PROCESSING

Based on standard Matlab package, JPEG images are loaded into MatLab and transformed into matrix form of size equivalent to camera detector size. As our primary concern is gradient based image processing [14], exact temperature interpretation is not essential as gradient method enables locating zones of interest without need for exact temperature level. First step is to read image to the Matlab and turn it to the greyscale image.

```
B=imread('thermal_image.JPG');
C=rgb2gray(B);
```

Thermal gradient [14] is obtained as

$$\text{grad } T = (\partial T / \partial x, \partial T / \partial y), \quad (1)$$

where x, y are horizontal and vertical directions of a pixel position in the pixel map. Gradient function flattens differences in thermal field with lower gradient values, while keeping visible zones with higher thermal gradient. The result is a clear image of transition zones between anomalies and undamaged structure. Significant advantage of gradient based method is elimination of unequal heating influences and background reflections, what is a common problem in active thermography. In Matlab, following command calculates thermal gradient.

```
[Gx, Gy] = imgradientxy(C);
G=Gx+Gy;
```

After the gradient matrix is created, matrix is exported to a JPEG image that enables visual interpretation of thermograms and location of anomalies.

```
imagesc(G);
```

3. COMPARISON OF MW AND LW PT IMAGES

To evaluate gradient based image processing, when applied on different wavelengths, comparison is made between cooled MW InSb Flir SC 5000 camera (resolution 320x256 pixels, sensitivity 0.02°C) and bolometric cameras Flir E60 (resolution 320x240 pixels, sensitivity 0.05°C) and Flir i7 (resolution 140x140 pixels, sensitivity 0.1°C). Thermal pulse is generated by preheating specimens with 1kW halogen lamp on 40 cm of distance and 2 min duration of preheating. Images are taken just after turning off and removing lamp from specimen. Emissivity coefficients are: 0.98 for uncoated

GRP in MW spectrum, 0.975 for coated GRP in MW spectrum, 0.95 for coated and uncoated GRP in LW spectrum.



Figure 1 Experimental setup

To compare different wavelengths and characteristics of thermal cameras, vacuum cured glass reinforced polymer (GRP) specimen is used (97 x 97 x 10.5 mm) [17]. To evaluate sensitivity specimen has several blind holes (diameter of 5 and 10 mm) with variable depth (2, 4, 6 and 8 mm) and two channels (5 and 10 mm width) with variable depth (0 to 10.4 mm).

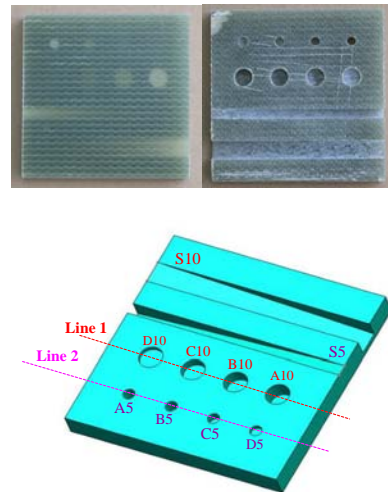


Figure 2 GRP vacuum cured test specimen with machined anomalies

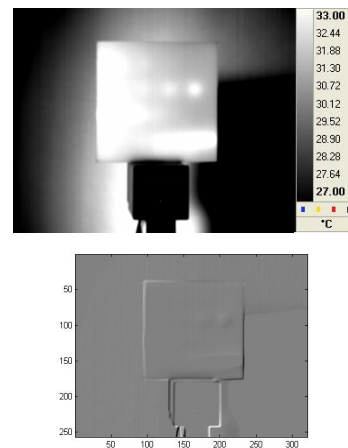


Figure 3 Thermal image (up) and gradient (down) acquired by MW 320x256/0.02°C camera

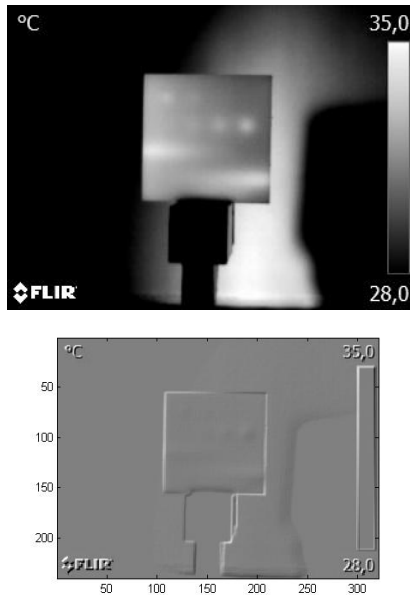


Figure 4 Thermal image and gradient acquired by LW 320x240/0.05°C camera

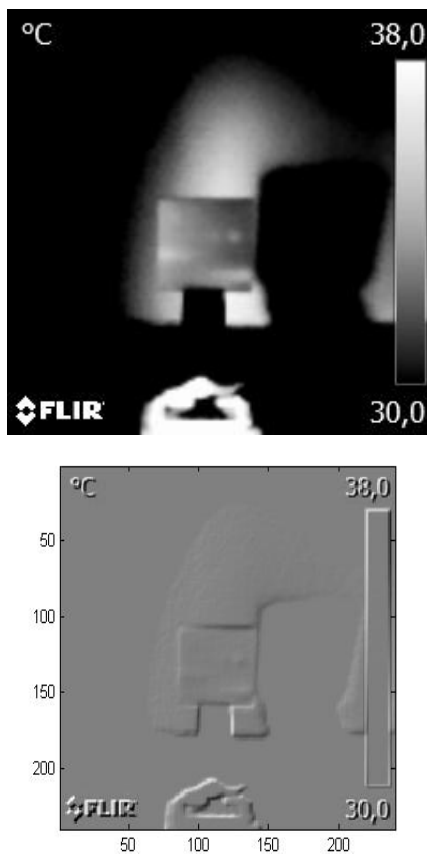


Figure 5 Thermal image and gradient acquired by LW 140x140/0.1°C camera

All presented IR images (Figures 3 to 5) are taken from unmachined side. Cameras are kept at the same distance, where different lenses influenced the specimen image size. MW 320x256/0.02°C camera has narrowest lens (25 mm / 1:3.0), LW 320x240/0.05°C has 25°x19° lens and LW 140x140/0.1°C has widest 29°x29° lens. Thermal images are as grayscale images loaded to Matlab and converted to the grayscale matrix.

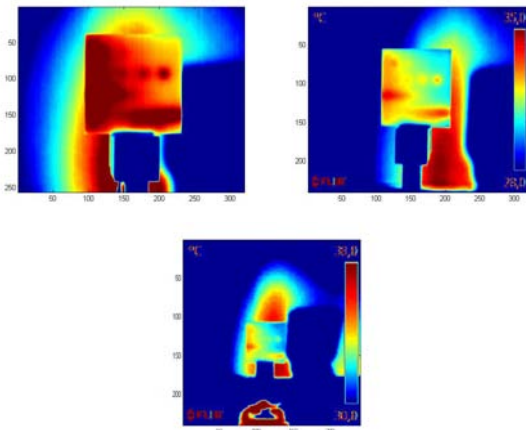


Figure 6 Matlab Colour scale for 320x256/0.02°C MW, 320x240/0.05°C LW and 140x140/0.1°C LW thermal image

To compare sensitivity, grayscale level is displayed across lines 1 and 2 crossing over blind holes and compared with line 3 crossing in between, i.e. area with no anomalies (Figure 2). Sensitivity (grayscale contrast) is defined as difference between lines L1, L2 and line L3. Blind Ø10 holes are named with letters A10 (deepest) to D10 (shallowest), while Ø5 holes are named with letters A5 (deepest) to D5 (shallowest).

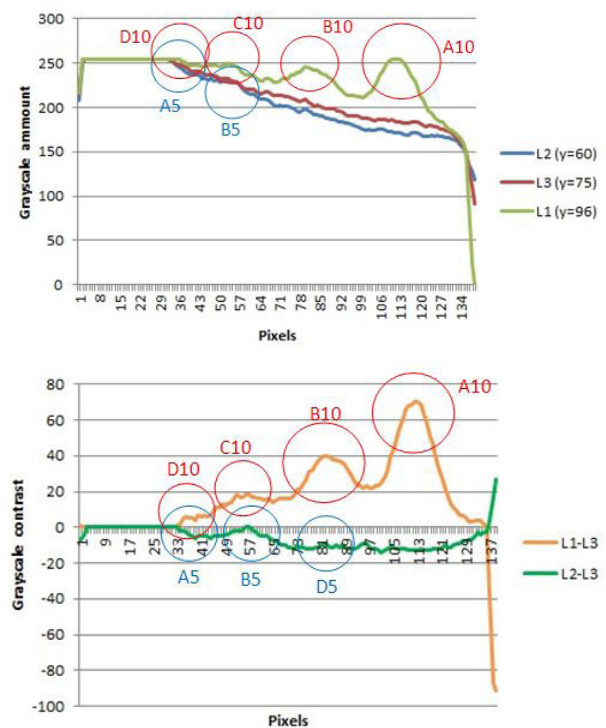


Figure 7 Grayscale level (up) and grayscale contrast (down) acquired by 320x256/0.02°C MW camera

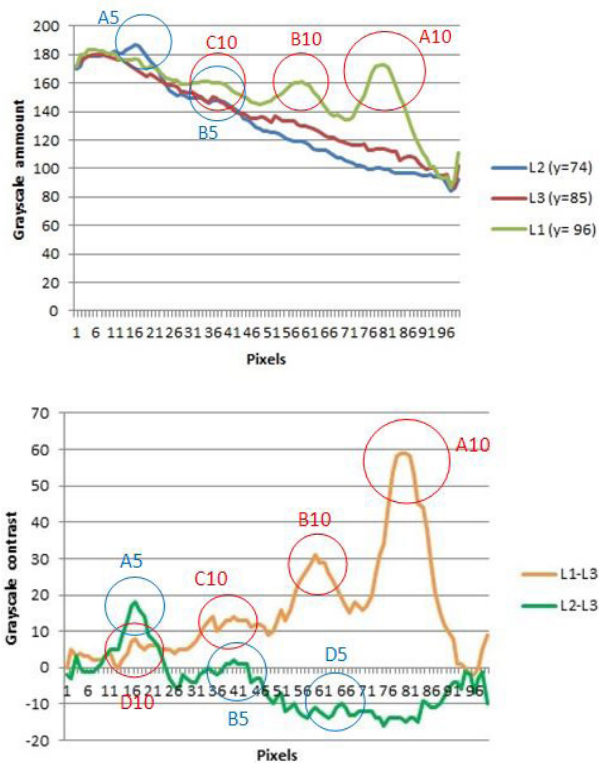


Figure 8 Grayscale level and contrast acquired by 320x240/0.05°C LW camera

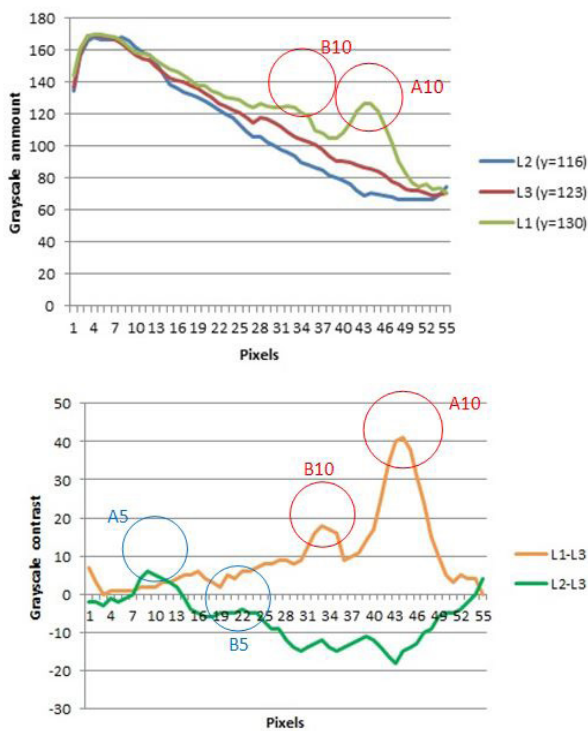


Figure 9 Grayscale level and contrast acquired by 140x140/0.1°C LW camera

Both LW cameras are showing very good sensitivity in comparison to MW cooled camera, proving the applicability of gradient based pulsed thermography method to the LW spectrum.

Comparison of wavelengths and cameras has been made for the specimen impacted with 19.61 J impactor [13] according to DIN 6038.

GRP specimen, described in [17], has been preheated for 2 minutes. Gradient function is applied on greyscale images. Colour scale (images imported in Matlab and displayed with same scale, Figure 14) is giving too confusing images. Gradient method enables locating the damage for the case of the 320x256/0.02°C MW and 320x240/0.05°C LW camera. 140x140/0.1°C LW camera is not giving clear result. When comparing all images, it can be concluded that method is not dependent on wavelength, but it is influenced by sensitivity and resolution of the camera itself, what is this case is low pixel size and sensitivity of 140x140/0.1°C LW camera. On the right side of specimen is the black PVC insulation tape used for comparing emissivity.



Figure 10 Impacted specimen

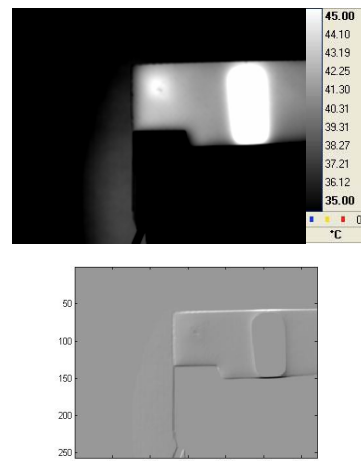


Figure 11 Thermal image and gradient acquired by 320x256/0.02°C MW camera

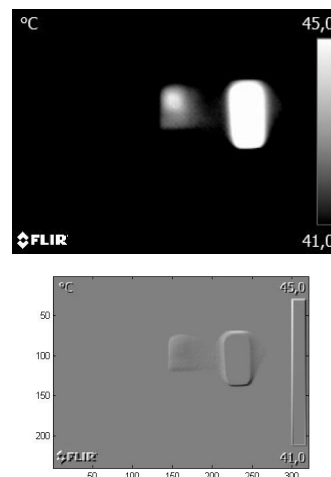


Figure 12 Thermal image and gradient (320x240/0.05°C LW camera)

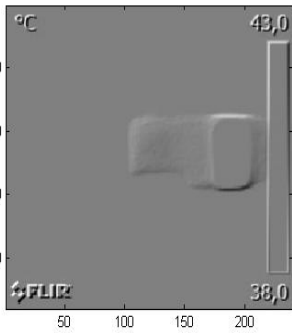
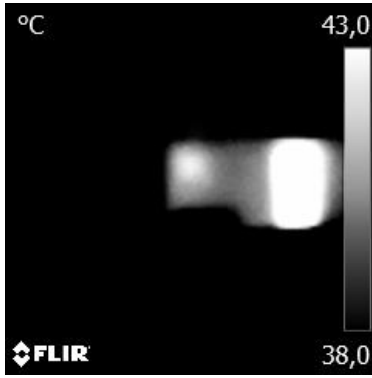


Figure 13 Thermal image and gradient (140x140/0.1°C LW camera)

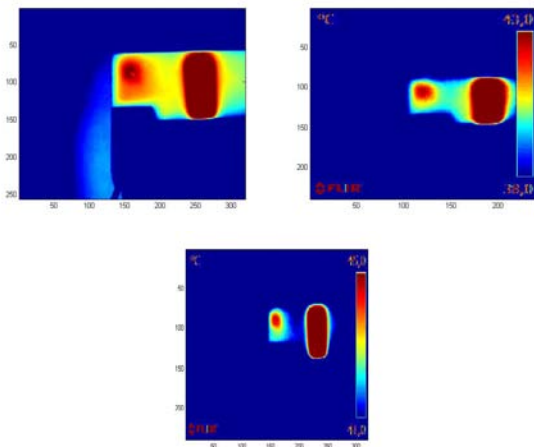


Figure 14 Colour scale for 320x256/0.02°C MW, 320x240/0.05°C LW and 140x140/0.1°C LW thermal image

Comparison has been made on example of impacted and severely delaminated specimen where delaminated zones are detectible on all cameras. Only MW camera gives clear image of zone where glass fiber rupture occurred. This example shoves clear benefit of MW cameras over LW cameras and evaluation limits when using LW cameras. Therefore, LW cameras can be used for detecting delamination zones, but LW cameras are not appropriate for detecting glass fiber ruptures. As in the example before, colored scale images are not so clear when performing NDT surveys (images are made after importing in Matlab).



Figure 15 Impacted and severely delaminated specimen

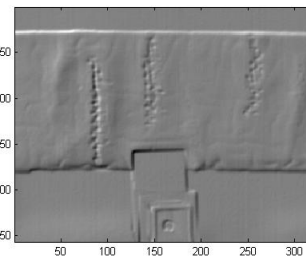
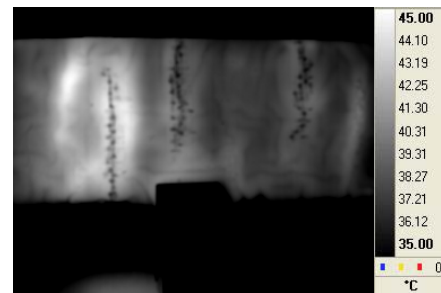


Figure 16 Thermal image and gradient acquired by 320x256/0.02°C MW camera

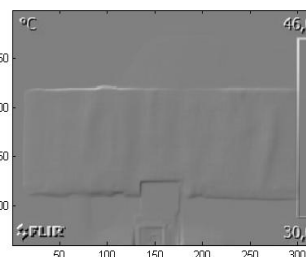


Figure 17 Thermal image and gradient acquired by 320x240/0.05°C LW camera

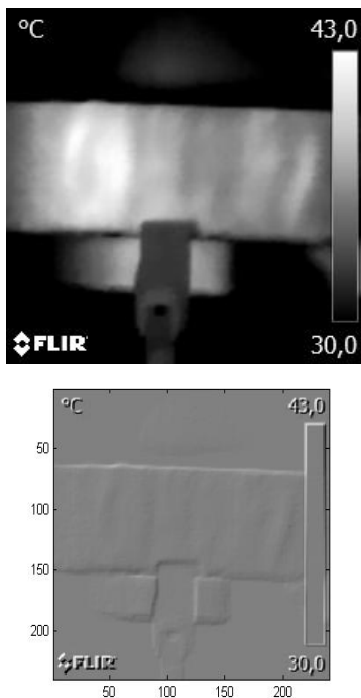


Figure 18 Thermal image and gradient acquired by 140x140/0.1°C LW camera

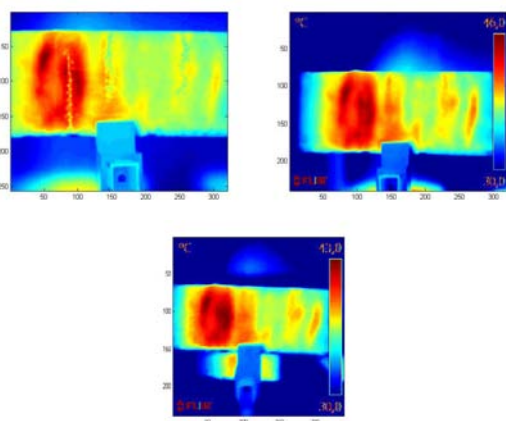


Figure 19 Colour scale thermal image for 320x256/0.02°C MW, 320x240/0.05°C LW and 140x140/0.1°C LW

4. THE APPLICATION OF GRADIENT BASED IMAGE PROCESSING ON FLOATING VEHICLES

Inspecting GRP boats is of particular interest due to the robustness and short inspection duration of IR based methods. Here some typical images of 20,5 m sailing boat survey and work-boat catamaran survey are demonstrating ability of IR thermography. First group of images shows IR (320x240/0.05°C LW) NDT survey of a 20,5 m sailing boat still under construction in the workshop (Figures 20 to 25).

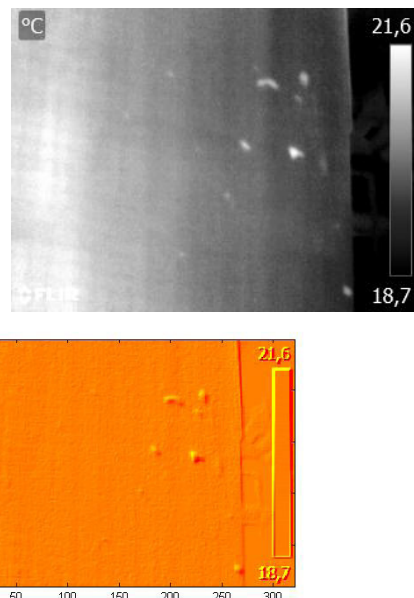


Figure 20 Air pockets in the gelcoat (image, thermal image and gradient)

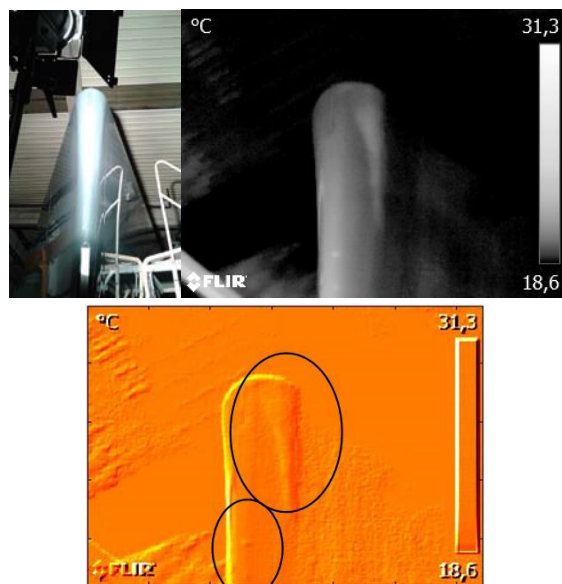


Figure 21 Air pockets and unequal gelcoat thickness in bow region

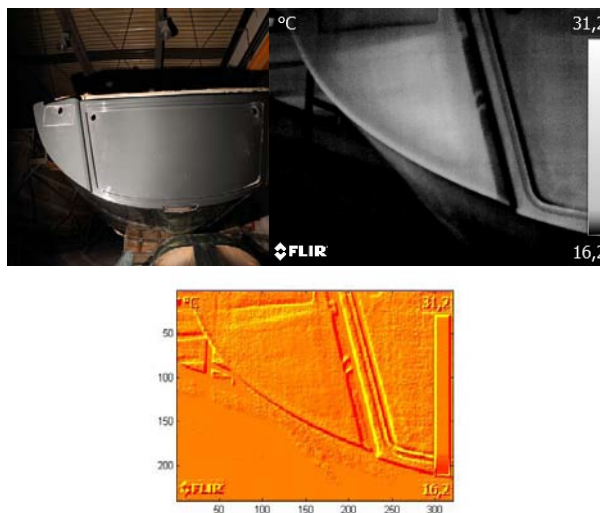


Figure 22 Detail of stern structure

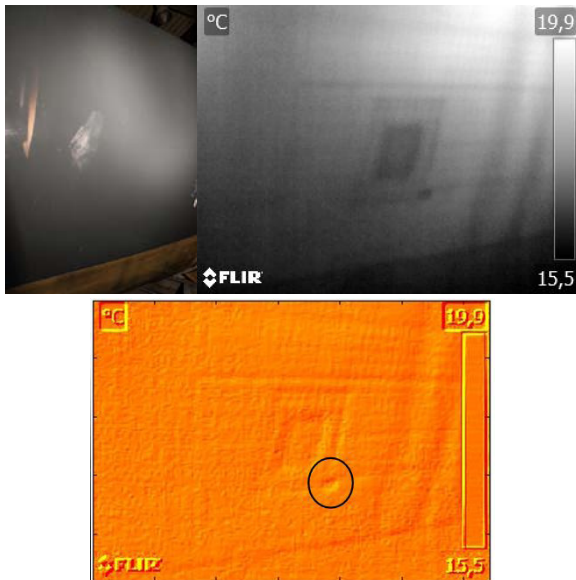


Figure 23 Resin inclusion near structural reinforcement

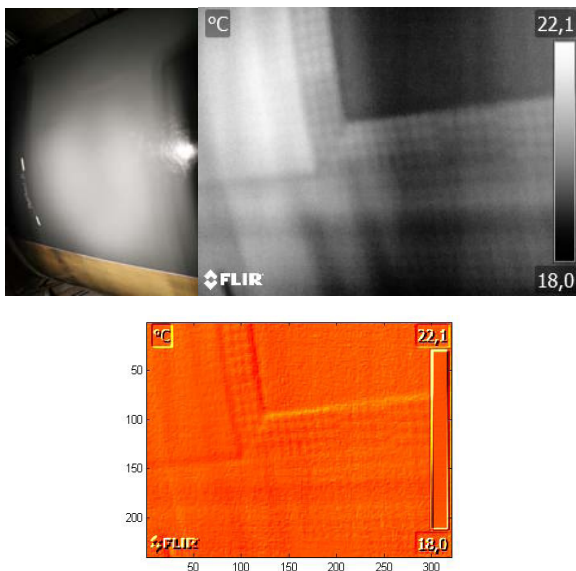


Figure 24 Confirmation and evaluation of structural reinforcement

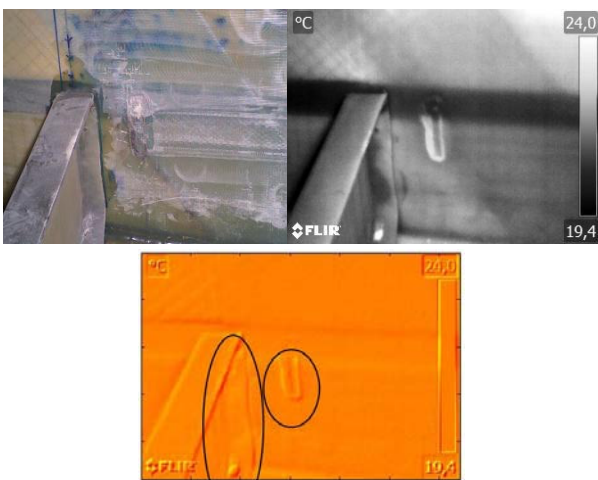


Figure 25 Improper bonding of reinforcement (left) and U form resin inclusion (right)

Application of gradient based image processing improves locating and validating anomalies, as well as inspecting structural details as reinforcements. Anomalies are visible on pure thermal images, but gradient method improves distinguishing anomalies from reflections and effects of unequal heating.

Last example (Figure 26) is a catamaran work-boat, where survey of crane structural support enabled locating delamination and cracks within GRP structure caused by misaligned flange reinforcement in clamping zone. Here IR (320x240/0.05°C LW) NDT survey was the base for properly reinforcing flange support and repairing GRP structure. Preheating time was here as well 2 minutes. Thermal image in Figure 26 is created as panoramic image from 5 thermal images (a Flir Tools plus software option).

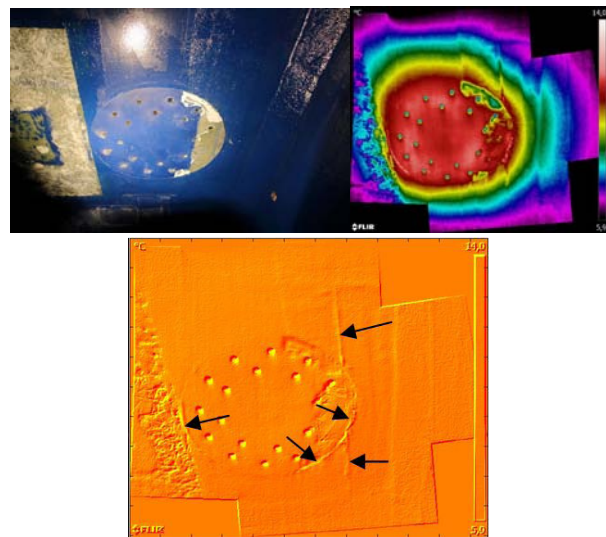


Figure 26 Debonding and fractures in GRP structure in the zone of flange support

5. CONCLUSION

Presented research proved that LW IR cameras can be used for NDT of GRP floating vehicles, expect the case when glass fibres rupture is considered. Method is robust, fast and applicable for MW and LW spectrum. Gradient based image processing eliminates reflections and influences of unequal heating. The presented image processing is not obtained from a raw image containing pixel-wise temperature distribution, but from a JPEG grayscale image. Such an approach enables image processing in academic research community without need for scientific camera software, supposing that standard Matlab software is available. Although

temperature amounts are lost, gradient based image processing is applicable to the grayscale images. As LW IR cameras are more and more in use, we hope that presented approach will help users entering the field of pulsed IR thermography, as a NDT method.

6. REFERENCES

- [1] Grispen, R.: Thermal imaging helps to detect water ingress in airplanes, Applications in maintenance and asset management, Maintworld 2, 2011.
- [2] Miller, B. F.: The feasibility of using thermography to detect subsurface voids in painted wooden panels. Journal of the American Institute for Conservatory, Vol. 16, Number 2, 27-35, 1977.
- [3] Ibarra-Castanedo, C.: Quantitative subsurface defect evaluation by pulsed phase thermog-raphy: Depth retrieval with the phase. Ph.D. thesis, Faculté des sciences et de génie, Université Laval, Québec, 2005.
- [4] Maladague, X., Galmiche, F., Ziadi, A.: Advances in pulse phase thermography. Infrared Physics & Technology, Vol. 43, 175-181, 2002.
- [5] Ibarra-Castanedo, C., González, D., Galmiche, F., Maldague, X. P., Bendada, A.: Discrete signal transforms as a tool for processing and analyzing pulsed thermographic data. Thermosense XXVIII, Vol. 6205, 2006.
- [6] Sakagami, T., Kubo, S.: Applications of pulse heating thermography and lock-in thermography to quantitative nondestructive evaluations. Infrared physics and Technology, 43, 211-218, 2002.
- [7] Carlomagno, G. M., Meola, C.: Comparison between thermographic techniques for frescoes NDT, NDT&E International 35 (2002) 559–565
- [8] Roche, J.M., Balageas, D.: Common tools for quantitative pulse and step-heating thermography-Part II: experimental validation. The 12th International Conference on Quantitative InfraRed Thermography (QIRT 2014), Jul 2014, BORDEAUX, France, 2014.
- [9] Milovanović, B., Banjad Pečur, I.: Detecting defects in reinforced concrete using the method of infrared thermography, HDKBR info, 11, 3-13, 2013.
- [10] Flir Application story series: FLIR thermal imaging cameras help detect material failures in bikes, www.flir.com
- [11] Flir Application story series: Advanced FLIR thermal imaging cameras help standardize testing of wind turbine blades, www.flir.com
- [12] Ullman, T. , Aoki, R., Schmidt, T.: Lock-in Thermography for Process Integrated Non-Destructive Evaluation of Carbon Fibre Reinforced Aircraft Structures. 10th International Conference on Quantitative InfraRed Thermography, July 27-20, Quebec, Canada, 2010.
- [13] Krstulović-Opara, L., Klarin, B., Neves, P., Domazet Ž.: Thermal imaging and Thermoelastic Stress Analysis of impact damage of composite materials. Engineering Failure Analysis, Vol. 18, 713–719, 2011.
- [14] Krstulović-Opara, L., Klarin, B., Garafulić, E., Domazet, Ž.: Application of gradient based IR thermography to the GRP structures inspection. Key Engineering Materials, Vols.488-489, 682-685, 2011.
- [15] Krstulovic-Opara, L., Domazet, Ž., Klarin, B., Garafulić, E.: The Application of IR Thermography to the NDT and Thermal Stress Analysis, HDKBR info, 6/7, 17-22, 2012.
- [16] Krstulović-Opara, L., Domazet, Ž., Garafulić, E.: Detection of osmotic damages in GRP boat hulls, Infrared Physics & Technology, Vol. 60, 359-364, 2013.
- [17] Garafulić, E. , Krstulović-Opara, L., Domazet, Ž.: Detection of material anomalies based on infrared thermography image processing, Proceedings of NDT week in Zagreb , 7.-12. October, Zagreb, Croatia, 3-13, 2013.